Optical properties of tungsten thin films perforated with a bidimensional array of subwavelength holes

Michaël Sarrazin and Jean-Pol Vigneron
Laboratoire de Physique du Solide, Facultés Universitaires Notre-Dame de la Paix, Rue de Bruxelles 61, B-5000 Namur, Belgium
(Received 6 February 2003; published 11 July 2003)

We present a theorical investigation of the optical transmission of a dielectric grating carved in a tungsten layer. For appropriate wavelengths tungsten indeed shows a dielectric behavior. Our numerical simulation leads to theoretical results similar to those found with metallic systems studied in earlier work. The interpretation of our results rests on the idea that the transmission is correlated with the resonant response of eigenmodes coupled to evanescent diffraction orders.

DOI: 10.1103/PhysRevE.68.016603 PACS number(s): 42.79.Dj, 42.25.Fx, 42.25.Bs

For several years, the properties and technological applications of one- or two-dimensionnal metallic gratings have received growing interest. In 1998, Ebbesen *et al.* [1] reported on optical transmission experiments performed on periodic arrays of subwavelength cylindrical holes drilled in a thin metallic layer deposited on glass. These experiments renewed the motivation for investigating metallic gratings. Two attractive characteristics of their results are often cited: the transmission, which is a lot higher than the addition of individual hole contributions, and the peculiar wavelength dependence of the transmission. Further work [1–7] has suggested that these features arise from the presence of the metallic layer and call for the presence of surface plasmons in order to explain these transmission characteristics. In particular, convex high transmission regions, i.e., regions between the minima, have been identified as regions dominated by the plasmon response. However, many questions remain and need to be answered in order to clarify the mechanisms involved in these experiments.

In a recent paper [8], extensive simulations were performed in order to understand the optical properties of a chromium layer similar to those developed in experiments. Recalling Wood's anomalies [9], it was shown that the transmission and reflection are better described as Fano's profiles correlated with the resonant response of the eigenmodes coupled to nonhomogeneous diffraction orders. Indeed, as explained by Fano [10] and by Hessel and Oliner [11] for one-dimensional gratings, Wood's anomalies are related to grating eigenmode excitation. To be accurate, they have shown that Wood's anomalies [11] may arise in two ways. The first case occurs at Rayleigh wavelengths, when a diffracted order becomes grazing to the grating plane [12]. The diffracted beam intensity then increases just before the diffracted order vanishes. The other case is related to a resonance effect. Such resonances come from coupling between the incident light and the eigenmodes of the grating. The two types of anomalies may occur separately and independently, or may almost coincide.

In our previous paper [8], as we used metal in our device, it seemed natural to assume that these resonances are surface plasmons. Nevertheless, it is important to note that our analysis did not make any hypothesis about the origin of the eigenmodes. This implies that it could be possible to obtain transmission curves similar to those found for metals, by substituting guided modes or other types of polaritons for the surface plasmons. This would allow one, for instance, to substitute dielectric guided modes for metallic excitations. This is the purpose of the present paper. We could also use films made of ionic crystals in the far infrared, and deal with phonon-polaritons (work in progress).

In this paper we report simulations of a device which consists of arrays of subwavelength cylindrical holes in a tungsten layer deposited on glass substrate (Fig. 1). Indeed, tungsten becomes dielectric on a restricted domain of wavelength in the range 240–920 nm, i.e., the real part of its permittivity becomes positive. The permittivity values are taken from experiments [13]. So, whereas plasmons cannot exist, we show that the transmission pattern is similar to that obtained in the case of a metallic film. However, experiment has also shown that a germanium film is not able to give rise to an Ebbesen effect. We then also need to explain here why in the case of germanium nothing interesting can be observed.

Our simulations rest on a coupled mode method (which takes into account the periodicity of the device permittivity) associated with the use of the scattering matrix formalism [8,14]. In this way, we calculate the amplitudes of the reflected and transmitted fields, for each diffracted order (which corresponds to a vector $\vec{g}$ of the reciprocal lattice), according to their polarization (s or p). In the following, for a square grating of parameter a, note that $\vec{g}=(2\pi/a)(i,j)$, so that the pair of integers (i,j) denotes the corresponding vector of the reciprocal lattice (i.e., diffraction order). In addition, we recall that the Rayleigh wavelength is defined as

$$\lambda_R^{u,i,j} = a\sqrt{\varepsilon_u}(i^2+j^2)^{-1/2}, \tag{1}$$

where ε_u represents the permittivity of either the vacuum (ε_v) or the dielectric substrate (ε_d). We calculate the zero transmission order, referring to the experimental measurements performed in the metallic case. We can also estimate the partial density of states (PDOS) for some positions in the first Brillouin zone.

The calculated transmission of the incident wave is shown against wavelength in Fig. 2(a) for the zero diffraction order, and for incident light normal to the surface of a W film on glass. The hole diameter is set to $d=320$ nm and the thick-

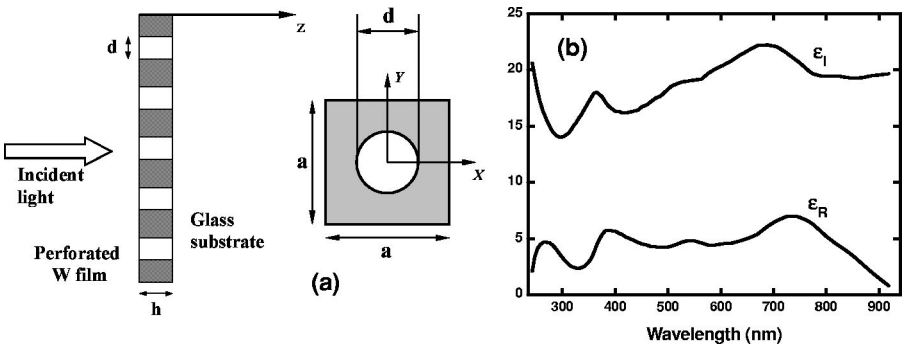

FIG. 1. (a) Diagrammatic view of the system under study. Transmission is calculated for the zeroth order and at normal incidence as in experiments. (b) Real and imaginary parts of tungsten permittivity.

ness of the film is $h=100$ nm. The transmission is given for square gratings of parameter $a=550$, 500, and 450 nm, respectively. In Fig. 2(a), it is shown that the transmission increases with the wavelength, and that it is characterized by minima marked 1 and 2 on the figure, which are located close after the Rayleigh wavelengths $\lambda_R^{d,0,\pm 1}$ and $\lambda_R^{v,0,\pm 1}$, respectively. The locations of these minima are shifted toward larger wavelengths when the grating size increases. Our investigations show that these minima disappear when considering a system without a hole. Note that these results are qualitatively similar to those from the experimental data of Ebbesen *et al.* in the case of metallic layers [1,2].

Figure 2(b) shows the calculated zero-order transmission as a function of the incident wavelength, for gratings with differents hole diameters. As in the case of metallic gratings [1,2,6,7], it is clear that the transmission curve does not depend on the hole diameter except for the amplitude of the spectral features.

In order to underline the correlation between the transmission amplitude and the hole diameter we also give in Fig. 2(c) the transmission amplitude for many hole diameter values [dots in Fig. 2(c)]. The transmission values are those which correspond to the maximum located at 576.7 nm for a square grating of parameter $a=500$ nm, with the chosen thickness of the film ($h=100$ nm). We show that the transmission amplitude increases exponentially as a function of the hole diameter [solid line in Fig. 2(c)]. This result suggests that there is no cavity mode involved in these phenomena.

In Fig. 2(d) we give the calculated transmission as a function of the wavelength of the incident wave for the zeroth diffraction order, for different layer thicknesses. As in the case of metallic gratings [1,2,6,7], we show that the behavior of the transmission curves does not depend on the thickness except for the overall amplitude.

The results we show in Fig. 2 present behaviors very similar to those obtained with metals [1,2], even though we used tungsten in its dielectric domain. Let us discuss this point. As explained in [8], the eigenmodes of the grating play a crucial role in these experiments. Let us first recall that the reflected and transmitted amplitudes are linked to the incident field through the S scattering matrix. Let us define F_{scat} as the scattered field and F_{in} as the incident field. Then, F_{scat} is related to F_{in} via the scattering matrix, in such a way that

$$S(\lambda)F_{in}(\lambda)=F_{scat}(\lambda). \tag{2}$$

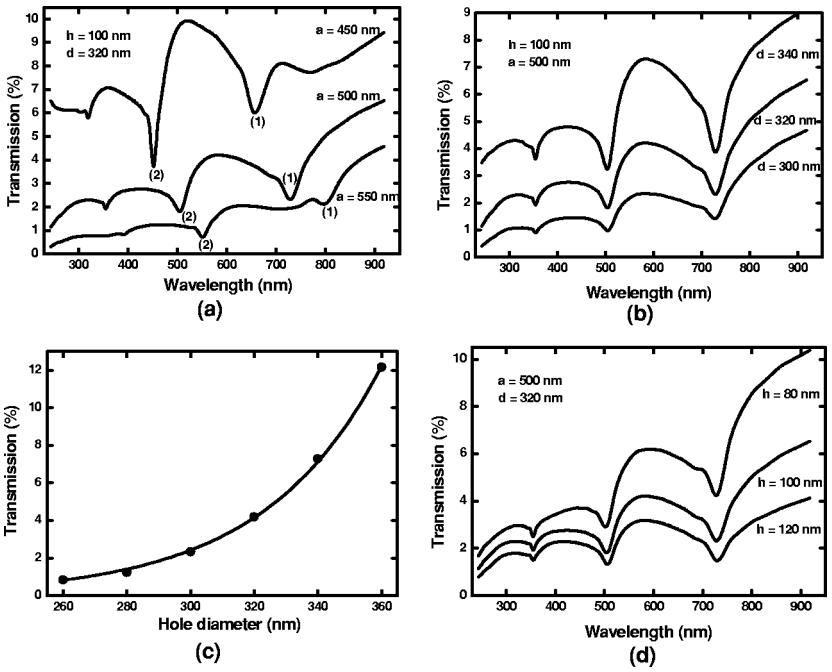

FIG. 2. Percentage transmission of the incident wave on the surface against wavelength, for the zeroth diffraction order, for different parameters of the square grating (a), for different hole diameters (b), and for different thicknesses (d). (c) represents the transmission vs hole diameter for a given wavelength.

In this way, the eigenmodes of the structure are solution of Eq. (2) which exist in the absence of the source, i.e., when

$$S^{-1}(\lambda_\eta)F_{scat}(\lambda_\eta)=0. \tag{3}$$

This homogeneous problem is well known in the theory of gratings [8,11]. Complex wavelengths $\lambda_\eta=\lambda_\eta^R+i\lambda_\eta^I$ for which Eq. (3) has nontrivial solutions require that

$$\det[S^{-1}(\lambda_\eta)]=0, \tag{4}$$

so that they coincide with the poles of the complex function $\det[S(\lambda)]$.

If we extract the singular part of S corresponding to the eigenmodes of the structure, we can write S as [8,11]

$$S(\lambda)=\sum_\eta \frac{R_\eta}{\lambda-\lambda_\eta}+S_h(\lambda), \tag{5}$$

i.e., in the form of a generalized Laurent series, where R_η is the residue associated with the pole λ_η and $S_h(\lambda)$ is the holomorphic part of S, which corresponds to a physically nonresonant process.

Thus, assuming that $f(\lambda)$ is the mth component of $F_{scatt}(\lambda)$, we have, for the expression for $f(\lambda)$ in the neighborhood of one pole λ_η [8,10,11],

$$f(\lambda)=\frac{r_\eta}{\lambda-\lambda_\eta}+s(\lambda), \tag{6}$$

where $r_\eta=[R_\eta F_{in}]_m$ and $s(\lambda)=[S_h(\lambda)F_{in}]_m$.

We consider the case where nonresonant processes cannot be neglected and assume that $s(\lambda)\sim s_0$ is a constant value. Thus, it is easy to show that Eq. (6) can be written as [8,11]

$$|f(\lambda)|^2=\frac{(\lambda-\lambda_z^R)^2+\lambda_z^{I2}}{(\lambda-\lambda_\eta^R)^2+\lambda_\eta^{I2}}|s_0|^2 \tag{7}$$

with

$$\lambda_z^R=\lambda_\eta^R-\nu^R \quad \text{and} \quad \lambda_z^I=\lambda_\eta^I-\nu^I, \tag{8}$$

where

$$\nu=\frac{r_\eta}{s_0}. \tag{9}$$

The coefficient ν measures the significance of the resonant effect, compared with nonresonant contributions. $\lambda_z=\lambda_z^R+i\lambda_z^I$ denotes the zero of Eqs. (6) and (7). This last expression takes into account the interferences between resonant and nonresonant processes, which lead to asymmetric transmission profiles. Equation (7) leads to a typically resonant process (described by a Lorentzian curve) or to a typical asymmetric behavior where a minimum follows a maximum, and vice versa, depending on the values of ν. We note that these properties, which result from the interference between resonant and nonresonant processes, are similar to those described by Hessel and Oliner [11] and by Fano [10]. Profiles like those describe in Fig. 3(a) are often referred to as ''Fano profiles.''

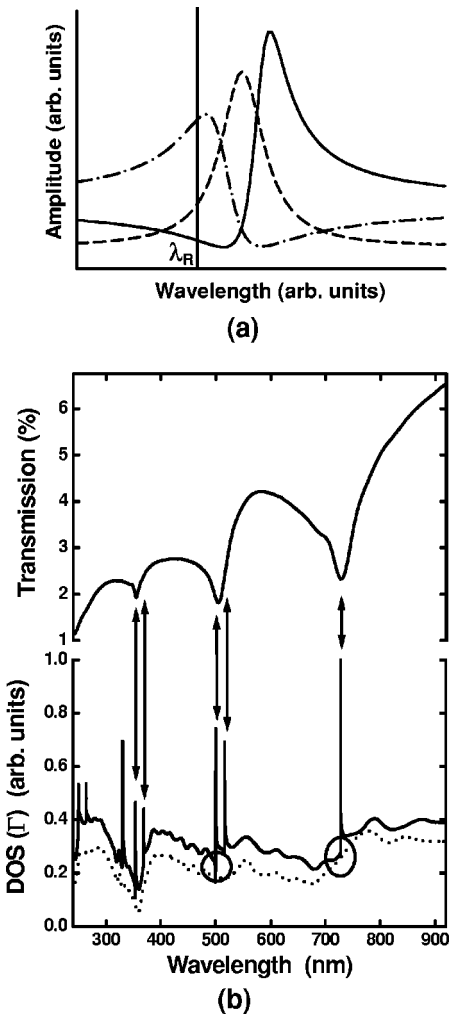

FIG. 3. (a) Representation of typical Fano profiles. (b) PDOS vs wavelength compared with transmission.

It is now necessary to find the structure eigenmodes. For this purpose, we show in Fig. 3(b) the partial density of states, i.e., the density of states at the center Γ of the first Brillouin zone. Indeed, when the incident light is normal to the surface, our assumption is that the density of states (DOS) at Γ is the dominant contribution to these phenomena.

The solid line shows the partial DOS that is calculated in the case of a grating with $d=320$ nm, $h=100$ nm, and $a=500$ nm. The dashed line shows the partial DOS that is calculated for a similar system in the absence of holes. The overall pattern of the partial DOS of the grating is related to the pattern of the partial DOS of the planar tungsten layer. Some sharp localized peaks appear, related to the eigenmodes of the tungsten grating. Such eigenmodes can be associated with guided modes of the tungsten grating only by assuming its dielectric properties. We note the Rayleigh anomalies (circles around sharp minima of the DOS) which appear just on the side of the eigenmodes at shorter wavelength. We also show the corresponding transmission for the

sake of comparison. One clearly notices the absence of coincidence between the position of the eigenmodes and the transmission maxima. Nevertheless, the eigenmodes are behind the typical profiles of the transmission curves [8]. In fact, one can interpret the features' line shapes as arising from resonant Wood's anomalies, similar to those studied by Fano [10] and by Hessel and Oliner [11].

Let us consider an incident propagative wave, which diffracts and generates an evanescent diffraction order. Such an order is coupled with a guided eigenmode which is characterized by a complex wavelength λ_η. It becomes possible to excite this eigenmode, which leads to a feedback reaction on the evanescent order. For this reason, Hessel and Oliner called such an order a ''resonant order.'' This process is related to the resonant term.

The evanescent resonant order can diffract due to the layer corrugation, and generates a contribution to the propagative zero diffraction order. Thus, one can ideally expect to observe a resonant (Lorentzian) profile for the zero diffraction order. Nevertheless, it is necessary to take into account a nonresonant diffraction process related to the holomorphic term of the scattering matrix. So the incident wave generates a propagative zero order. Then, one takes into account the interference of two rates, i.e., the resonant and nonresonant contributions to order zero. Profiles appear that are typically the Fano profiles which correspond to resonant process where one takes into account nonresonant effects. One notes that a maximum in transmission does not necessarily correspond to the maximum of resonance of a diffraction order. So, the Fano profile behavior of the transmission results from superimposing resonant and nonresonant contributions to the zero diffraction order.

If one refers to the present situation, the resonance is close to the Rayleigh wavelength. Consequently, the asymmetric Fano profiles are shifted toward the Rayleigh wavelength in the same way. Then the transmission minima, which in fact correspond to minima of the Fano profile, disappear when crossing a Rayleigh wavelength. The maxima of the transmission, which are shifted toward larger wavelengths as shown in [8], correspond to the maxima of the Fano profile.

Thus the maxima do not correspond explicitly to maxima of resonances but rather to the maxima of the Fano profile originating from the excitation of guided modes and not surface plasmons as in the metallic case [8]. Nevertheless, it is necessary to emphasize why in the case of germanium, which is a dielectric, nothing similar has been observed. In fact, in the wavelength domain of our simulations, the imaginary part of the tungsten permittivity is large, whereas in the case of germanium, in the domain wavelength studied by Ebbesen *et al.*, the imaginary part of the permittivity is weak enough to consider germanium as transparent. In this situation, the contribution of the holomorphic part of the scattering matrix is much larger than that of the resonant part so that the latter can be neglected. Thus one completely loses the benefit of the resonant effects which play a fundamental role in the transmission line shapes. Moreover, in the case of tungsten, the opacity is such that there is not enough direct transmitted light to mask the effects of resonant processes.

It would be desirable to obtain more experimental data about tungsten gratings, as a way to confirm our theorical findings. The ability to use dielectric layers would open the potential for Ebbesen devices. One notes that the role of guided resonances and Fano profiles in photonic crystal slabs has also been underlined by Fan and Joannopoulos in a recent paper [15].

The authors thank J.-M. Vigoureux and D. Van Labeke for their invaluable advice and useful discussions. We acknowledge the use of Namur Scientific Computing Facility (Namur-SCF), a common project between the FNRS, IBM Belgium, and the Facultés Universitaires Notre-Dame de la Paix (FUNDP). This work was carried out with support from EU5 Center of Excellence (Grant No. ICAI-CT-2000-70029) and from the Inter-University Attraction Pole (Grant No. IUAP P5/1) on ''Quantum-Size Effects in Nanostructured Materials'' of the Belgian Office for Scientific, Technical, and Cultural Affairs.

[1] T.W. Ebbesen, H.J. Lezec, H.F. Ghaemi, T. Thio, and P.A. Wolff, Nature (London) **391**, 667 (1998).
[2] H.F. Ghaemi, T. Thio, D.E. Grupp, T.W. Ebbesen, and H.J. Lezec, Phys. Rev. B **58**, 6779 (1998).
[3] U. Schröter and D. Heitmann, Phys. Rev. B **58**, 15 419 (1998).
[4] J.A. Porto, F.J. Garcia-Vidal, and J.B. Pendry, Phys. Rev. Lett. **83**, 2845 (1999).
[5] D.E. Grupp, H.J. Lezec, T.W. Ebbesen, K.M. Pellerin, and T. Thio, Appl. Phys. Lett. **77**, 1569 (2000).
[6] T. Thio, H.J. Lezec, and T.W. Ebbesen, Physica B **279**, 90 (2000).
[7] A. Krishnan, T. Thio, T.J. Kim, H.J. Lezec, T.W. Ebbesen, P.A. Wolff, J. Pendry, L. Martin-Moreno, and F.J. Garcia-Vidal, Opt. Commun. **200**, 1 (2001).
[8] M. Sarrazin, J.-P. Vigneron, and J.-M. Vigoureux, Phys. Rev. B **67**, 085415 (2003).
[9] R.W. Wood, Phys. Rev. **48**, 928 (1935).
[10] V.U. Fano, Ann. Phys. (Leipzig) **32**, 393 (1938).
[11] A. Hessel and A.A. Oliner, Appl. Opt. **4**, 1275 (1965).
[12] Lord Rayleigh, Proc. R. Soc. London, Ser. A **79**, 399 (1907).
[13] D.W. Lynch and W.R. Hunter, in *Handbook of Optical Constants of Solids II*, edited by E.D. Palik (Academic, New York, 1991).
[14] J.P. Vigneron, F. Forati, D. André, A. Castiaux, I. Derycke, and A. Dereux, Ultramicroscopy **61**, 21 (1995).
[15] S. Fan and J.D. Joannopoulos, Phys. Rev. B **65**, 235112 (2002).